



# Can seafloor voltage cables be used to study large-scale circulation? An investigation in the Pacific Ocean.

Neesha R. Schnepf<sup>1,2</sup>, Manoj C. Nair<sup>1,2</sup>, Jakub Velínský<sup>3</sup>, and Natalie P. Thomas<sup>4</sup>

<sup>1</sup>Cooperative Institute for Research in Environmental Sciences (CIRES), University of Colorado, Boulder, CO, USA

<sup>2</sup>National Centers for Environmental Information, National Oceanic & Atmospheric Administration, Boulder, CO, USA

<sup>3</sup>Department of Geophysics, Faculty of Mathematics and Physics, Charles University, Praha, Czech Republic

<sup>4</sup>Department of Atmospheric and Oceanic Science, University of Maryland, College Park, MD, USA

**Correspondence:** Neesha R. Schnepf (neesha.schnepf@colorado.edu)

**Abstract.** Marine electromagnetic (EM) signals largely depend on three factors: flow velocity, Earth's main magnetic field, and seawater's electrical conductivity (which depends on the local temperature and salinity). Because of this, there has been recent interest in using marine EM signals to monitor and study ocean circulation. Our study utilizes voltage data from retired seafloor telecommunication cables in the Pacific Ocean to examine whether such cables could be used to monitor circulation velocity or transport on large-oceanic scales. We process the cable data to isolate the seasonal and monthly variations, and evaluate the correlation between the processed data and numerical predictions of the electric field induced by ocean circulation. We find that the correlation between cable voltage data and numerical predictions strongly depends on both the strength and coherence of the velocities flowing across the cable, as well as the length of the cable. The cable within the Kuroshio Current had the highest correlation between data and predictions, whereas two of the cables in the Eastern Pacific gyre— a region with both low flow speeds and interfering velocity directions across the cable— did not have any clear correlation between data and predictions. Meanwhile, a third cable also located in the Eastern Pacific gyre had modest correlation between data and predictions— although the cable is very long and the speeds were low, it was located in a region of coherent flow velocity across the cable. While much improvement is needed before utilizing seafloor voltage cables to study and monitor oceanic circulation across wide regions, we believe that with additional work, the answer to our title's question may eventually be yes.

## 1 Introduction

Evaluating and predicting the ocean state is crucially important for reconciling and mitigating climate change's impact on our planet. Oceanic electromagnetic (EM) signals may be directly related to physical parameters of the ocean state, including flow velocity, temperature, and salinity. This has been known for centuries: in 1832, Michael Faraday was the first to attempt an experiment of measuring the voltage induced by the brackish water of the Thames River (Faraday, 1832). His study was not



very successful, but since then, marine EM signals have been detected by both ground and satellite measurements (Larsen, 1968; Malin, 1970; Sanford, 1971; Cox et al., 1971; Tyler et al., 2003; Sabaka et al., 2016).

Marine electromagnetic fields are produced because saline ocean water is a conducting fluid with a mean electrical conductivity of  $\sigma = 3 - 4 \text{ S m}^{-1}$ . As this electrically conductive fluid passes through Earth's main magnetic field ( $\mathbf{F} \approx 20 - 70 \mu\text{T}$ ), it induces electric fields, electric currents, and secondary magnetic fields. The electric current produced by a specific oceanic flow depends on the flow's velocity, the Earth's main magnetic field, and the seawater electrical conductivity, which in turn depends on salinity and temperature. Thus, ideally, three physical oceanic parameters could be extracted from marine EM studies: velocity, salinity, and temperature. However, extracting multiple parameters would require using multiple oceanic electromagnetic signals (eg. the signals from multiple tidal modes, and perhaps also from circulation) (Irrgang et al., 2017; Schnepf, 2017).

In practice, velocity is the only quantity so far determinable from marine EM data. This was accomplished using a passive seafloor telecommunications cable which recorded the voltage difference between Florida and Grand Bahama Island, a distance of approximately 200 km (Larsen and Sanford, 1985; Larsen, 1991, 1992; Baringer and Larsen, 2001). As the Florida Current passed over the cable, a voltage was induced and this voltage was directly related to the depth-integrated velocity across the cable (i.e. they determined the transport volume). Since 1985, the National Oceanic and Atmospheric Administration (NOAA) has been using submarine cables to monitor the transport of the Florida Current through the Strait of Florida.

While data from seafloor voltage cables have been used to study a variety of geopotential fields (Lanzerotti et al., 1986, 1992a; Chave et al., 1992; Shimizu et al., 1998; Fujii and Utada, 2000; Lanzerotti et al., 2001), NOAA's work in the Strait of Florida is the only case of a seafloor voltage cable being reliable to determine the overlying oceanic flow. Numerical work suggests that cables spanning larger regions should still strongly correlate to the flow velocities (Flosadóttir et al., 1997; Vanyan et al., 1998; Manoj et al., 2010), however, there are many challenges in using longer cables. These challenges are largely due to the myriad of processes which may also induce marine electromagnetic fields, especially across the length of the cable: secular variation (Shimizu et al., 1998), variations in ionospheric tides (Pedatella et al., 2012; Schnepf et al., 2018), geomagnetic storms or longer period ionospheric/magnetospheric signals (Lanzerotti et al., 1992a, 1995, 2001).

This study aims to provide a 'first step' answer to the question can seafloor voltage cables be used to study large-scale circulation? We evaluate the correlation between data from large-scale seafloor voltage cables and numerical predictions of the electric field induced by ocean circulation to discuss whether it may eventually be feasible to use large-scale cables for monitoring ocean flows. In the following section, we detail the seafloor voltage cables and data processing techniques utilized in this study. This section is followed by an explanation of our numerical predictions, then a discussion of the results and conclusions.

## 2 Data and data processing

This study used hourly data from four seafloor voltage cables (detailed in Table 1): three retired AT&T cables (the HAW cables) and one cable managed by the University of Tokyo's Earthquake Research Institute (the OKI cable). The cables HAW1N and HAW1S are 3805 km long and run parallel to each other from Point Arena, California to Hanauma Bay, Hawaii. As



shown in Figure 1, the parallel cables have very similar data, providing a unique and helpful situation for testing the data  
55 processing methods and for comparing the observations to numerical predictions. These three cables have been used in previous  
studies, including those examining geopotential variations (Chave et al., 1992; Lanzerotti et al., 1992b; Fujii and Utada, 2000),  
ionospheric phenomena (Lanzerotti et al., 1992a), oceanic tides (Fujii and Utada, 2000), and lithospheric/mantle electrical  
conductivity (Koyama, 2001).

The first step in processing the hourly data was the removal of geomagnetically noisy days (i.e., days where the geomagnetic  
60 Ap index was greater than or equal to 20; see Denig 2015 for more on the Ap index). This shrunk the amount of available  
data by 16.1%-21.6% for each cable. Next, to remove tidal signals the 12 dominant daily tidal modes were fit to the data via  
least-squares and then subtracted. Because the data sets have many gaps exceeding 24 hours in length (for example, see Figure  
2), the data was then smoothed using cubic splines. For seasonal variations, we used 90 day knots between splines, and for  
monthly variations, we used 30.5 days between knots. Although the daily variations should directly relate to barotropic wind-  
65 forced processes (Irrgang et al., 2016a, b, 2017), because of both the data's hourly time sampling and frequent data gaps, as  
well as challenges in producing daily numerical predictions, we chose to focus on monthly and seasonal variations. Each step  
of the data processing is shown in Figure 2.

A weakness of this data processing is that it does not prevent inclusion of induced signals due to seasonal changes in  
ionospheric electromagnetic tidal strength. While we removed tidal signals from a least-squares fit, we applied this fit to the  
70 entire dataset and did not attempt to remove seasonal changes in ionospheric tides. Seasonally, ionospheric electromagnetic  
tides can significantly change amplitude (Pedatella et al., 2012), and the horizontal components of these tides are likely to  
induce signals at the ground (Schnepf et al., 2018), however, attempting to constrain seasonal changes in tidal strength is  
challenging. Ideally, the least-squares fit could be conducted on shorter intervals of the data, but this worsens the accuracy of  
the least-squares inversion. Ionospheric field models could be used, but this would also introduce unknown error quantities.  
75 Thus, we did not attempt to remove seasonal changes in tidal amplitude but remind the reader that these signals may influence  
the monthly and seasonal variations.

### 3 Numerical predictions of ocean circulation's electric field

We numerically predict the electromagnetic signals produced by ocean circulation using the time-domain numerical solver  
elmTD of the electromagnetic induction equation (Velínský and Martinec, 2005; Velínský, 2013; Šachl et al., 2019; Velínský  
80 et al., 2019),

$$\mu_0 \frac{\partial \mathbf{B}}{\partial t} + \nabla \times \left( \frac{1}{\sigma} \nabla \times \mathbf{B} \right) = \mu_0 \nabla \times (\mathbf{u} \times \mathbf{F}). \quad (1)$$

Here  $\mathbf{B}(\mathbf{r}; t)$  is the induced magnetic field,  $\mathbf{u}(\mathbf{r}; t)$  is the velocity,  $\mu_0$  is the magnetic permeability of vacuum,  $\sigma(\mathbf{r}; t)$  is the  
electrical conductivity, and  $\mathbf{F}(\mathbf{r}; t)$  is the main geomagnetic field. The observable electric field  $\mathbf{E}(\mathbf{r}; t)$  is obtained from the  
induced magnetic field by post-processing,

$$85 \quad \mathbf{E} = \frac{1}{\mu_0 \sigma} (\nabla \times \mathbf{B}) - \mathbf{u} \times \mathbf{F}. \quad (2)$$



The elmgTD time-domain solver is based on spherical harmonic parameterization in lateral coordinates, and uses 1-D finite elements for radial discretization. The model is fully three-dimensional, incorporating also the vertical stratification of the ocean electrical conductivity and of the horizontal velocities, and accounting for the effect of variable bathymetry. Moreover, the seasonal variations of the ocean electrical conductivity, and the secular variations of the main field are taken into account. The solution includes both the poloidal and toroidal components of the induced magnetic field (Šachl et al., 2019; Velínský et al., 2019), thus allowing for the inductive and galvanic coupling between the oceans and the mantle, as well as self-induction within the oceans. Numerically, the linear system is solved by the preconditioned iterative BiCGStab(2) scheme (Sleijpen and Fokkema, 1993) with massive parallelization applied across the time levels.

Monthly values of the horizontal components of ocean velocity from the data-assimilated model Estimating the Circulation and Climate of the Ocean (ECCOv4r3) (Forget et al., 2015; Fukumori et al., 2017) were input into the elmgTD solver to compute the electromagnetic fields they induce from January 1997 to November 2001. Along with the monthly velocity values from ECCO, monthly values from the International Geomagnetic Reference Field (IGRF) (Finlay et al., 2010) were used for the main field and monthly climatological data from NOAA's World Ocean Atlas (WOA) were used to describe the global seawater electrical conductivity  $\sigma$  (Tyler et al., 2017). Figure 3 illustrates these inputs used for the elmgTD numerical solver. Underlying these inputs, the electrical conductivity of the mantle follows the 1-D global profile obtained by inversion of satellite data (Grayver et al., 2017).

In the present calculations, we truncate the spherical harmonic expansion at degree 240, corresponding to approximately  $0.75 \times 0.75$  degree resolution. The radial parameterization within the oceans uses 50 shell layers, following the irregular discretization of the ECCO model. The seawater monthly conductivities from NOAA's WOA were interpolated to the same grid via bilinear formula in angular coordinates, and weighted, conductance-preserving averaging in radius.

The model was run from January 1997 through the end of November 2001. Global results were extracted from the middle of every month (e.g., 1997-01-17, 1997-02-15, 1997-03-18, 1997-04-17, etc.), but daily results were extracted along the transect of the cables' paths. Figure 4 shows both the obtained electric field and the total applied forcing  $|\mathbf{u} \times \mathbf{F}|$  at the seafloor and sea surface. To compare numerical predictions with the processed seafloor cable observations, the seafloor electric field was isolated by determining the electric field values of the depth layer most closely corresponding to the seafloor. These seafloor electric field values were then integrated along the path of a given cable, excluding the cable's continental endpoints. The results of this are shown and discussed in the next section.

#### 4 Results & discussion

Figure 5 shows the processed cable data for both the 90-day knotted spline fit and the 30.5-day knotted spline fit (these are shown in black, with thinner lines denoting areas of data gaps). Plotted with the cable data are the results of the numerical prediction, both the predictions smoothed by a 90-day spline and a 30.5-day spline. Matlab's function 'corrcoef' was used to determine the correlation coefficients ( $R$ , shown in Table 2) between the processed data and numerical predictions. Negative correlation coefficients imply negative correlation and values close to 0 suggest weak correlation. The function 'corrcoef' also



calculates  $p$ -values corresponding to the correlation coefficients; all of the  $p$ -values were equal to 0, which suggests a reliable  
120 determination of  $R$ .

From the correlation coefficients,  $R^2$  values were also determined. These illustrate what percentage of the data may be explained by our numerical prediction. As shown in Table 2, the OKI cable had the highest  $R$  and  $R^2$  values: for the monthly variations, up to 35.05% may be explained by our model, whereas for seasonal variations, up to 42.59% may be explained by our model. Figure 5 shows the predicted OKI voltage values (shifted upwards by 1.8 V for plotting purposes) and the processed  
125 cable data. The 90-day knotted spline fit (Fig. 5a) shows good agreement in the timing of local minima/maxima up to 2001, after which the prediction has a local maxima concurrent with a local minima in the data. For the 30.5-day knotted spline fit (Fig. 5b), the prediction does not fully capture the three local maxima and two local minima of 1999, but it generally seems to follow the rest of the highs and lows. Given the relatively large ocean flow velocities in that region due to the Kuroshio Current (see Fig. 3a-b), the induced electric field and total forcing in the region of the OKI cable is much stronger than in other areas  
130 of the North Pacific Ocean (see Fig. 4), so it is expected that this cable would have both the greatest flow-induced signal within the cable data, as well as the best fit with the numerical predictions. Additionally, the OKI cable is much shorter than the HAW cables (it is less than 40% the length of those three Hawaii-to-California cables). The shorter length allows for an improved signal-to-noise ratio.

Opposite of the OKI cable, the HAW1N and HAW1S cables showed weak correlation between the processed cable data  
135 and the numerical predictions. This is evident in both Figure 5c-d and Table 2. The  $R$  values for both cables are negative, suggesting negative correlation, and range from -0.1540 to -0.3591. For the HAW1S cable's monthly and seasonal variations comparison,  $R^2$  values suggest the numerical prediction only explains  $\sim 2$ -3% of the data—percentages so low, it suggests our model effectively does not capture the data at all. For the HAW1N cable, the  $R^2$  values are slightly improved: for monthly variations,  $R^2$  is 7.16%, and for seasonal variations, it is 12.9%. While this poor correlation is unfortunate since these two  
140 cables were ideal in their parallel set-up, it is not unexpected considering the very weak ocean flow speeds within this region (see Fig. 3a-b). An additional challenge is that the zonal velocities across the HAW1N&S cables change directions—looking at Figure 3b, the surface velocities are negative near California, but positive westward along the cable towards Hawaii. Because the voltage measured by the cable depends on the integration of electric field along the cable, there likely are interfering signals that further minimize the cable's total induced signal. The large length of the cable also further worsens the signal-to-noise  
145 ratio.

The HAW3 cable lies a bit to the south of the HAW1N&S cables and it is also within the low speed region of the Eastern Pacific Gyre. Figure 5e-f illustrates that this cable's numerical predictions match the processed data marginally better than the HAW1N&S cables and HAW3 has modestly stronger correlation values than the HAW1N&S cables. For the monthly variations,  $R = 0.3129$  and  $R^2$  was 9.79%, and for the seasonal variations,  $R = 0.4111$  and  $R^2$  was 16.90%. As expected, due  
150 to the lower flow speeds and greater cable length, the correlation is weaker than for the OKI cable.

Larsen's (1992) studies evaluating transport in the Straight of Florida from seafloor voltage cable data had correlation squared values corresponding to much higher correlation than the correlation values of this study. As shown in Figure 20 of his paper, his correlation squared values ranged from 0.61 to 0.94. However, Larsen's study was fundamentally different: the seafloor



voltage cable was an order of magnitude shorter than the cables considered in this study and the Gulf Stream within the Strait  
155 of Florida has large speeds, as well as coherent velocities flowing perpendicularly to the cables, so Larsen's study overall had  
a more ideal signal-to-noise ratio.

For the cables connecting California and Hawaii, it would be interesting if instead of one cable that is almost 4000 km  
in length, multiple cables of shorter lengths were used. The surface velocity snapshots shown in Figure 3a-b show dominant  
velocity directions for different areas of the HAW cables. Using multiple cables of shorter length would not only improve the  
160 signal-to-noise ratio, but could also better capture this sort of velocity variability.

The OKI cable would likely have improved correlation between the processed data and numerical predictions if the cable  
was laying perpendicular to— rather than parallel to— the Kuroshio Current. This would induce the greatest possible electric  
current in the cable and further improve the cable's signal-to-noise ratio.

## 5 Conclusions

165 We present an evaluation of using seafloor voltage cables for monitoring circulation across oceanic basins. We compare pro-  
cessed seafloor voltage cable data with the numerical predictions produced using an electromagnetic induction solver, fed  
by flow velocity estimates from the data assimilated model ECCO and seawater electrical conductivity climatologies from the  
NOAA World Ocean Atlas. We find that the correlation between cable voltage data and numerical predictions strongly depends  
on both the amplitude and direction of the flow velocities across the cable.

170 While much improvement is needed before utilizing seafloor voltage cables to study and monitor ocean circulation across  
large regions, we believe that seafloor voltage cables can eventually be used to study and monitor large-scale ocean flow. The  
cables used in this study were installed for telecommunication purposes— there was no regard for whether these cables would  
be best suited to monitor ocean currents. Flow information can most reliably be extracted from seafloor voltage cable data  
when the flow has mostly unidirectional, perpendicular velocities across the cable. For our study, the OKI cable was in the  
175 area with the largest velocities, but because it is oriented mostly parallel to the Kuroshio Current, its correlation would likely  
greatly improve if it was instead perpendicular to the current's flow.

If voltage cables were strategically placed on the seafloor between Antarctica and Chile (a distance of  $\sim 700$  km), or Antarc-  
tica and New Zealand (a distance of  $\sim 1300$  km), because of both the shorter cable length (as compared to the HAW1 and  
HAW3 cables) and the relatively uniform and large flow velocities, the correlation between data and predictions could be quite  
180 high. Indeed, seafloor voltage cables may be a very effective method for measuring and continuously monitoring the flow of  
the Antarctic Circumpolar Current— this is definitely something worth investigating.

Using existing cables, the correlation between data and numerical predictions will likely also improve if methodology is  
enhanced to remove induced signals from seasonal variations in ionospheric signals.



185 *Data availability.* The data and numerical predictions discussed in this study are freely available for download at the website  
[geomag.colorado.edu/OCEM](http://geomag.colorado.edu/OCEM).

*Author contributions.* N. R. S. and M. N. conceived the questions and methodology of this study. N. R. S. and N. P. T. worked on the processing of cable data. N. R. S. was also responsible for comparing the processed data with the numerical results, as well as writing the manuscript with discussions and contributions from all the authors. M. N. supervised N. R. S. and N. P. T. on work related to this project and provided useful feedback on improving the manuscript. J. V. carried out the numerical work and also contributed to improving the  
190 manuscript.

*Acknowledgements.* N. R. S. was supported by NASA grant 80NSSC17K0450. N. R. S. and M. N. were also supported by a CIRES IRP grant. J.V. acknowledges the support of the Grant Agency of the Czech Republic, project No. P210/17-03689S. The computational resources were provided by The Ministry of Education, Youth and Sports, Czech Republic, from the Large Infrastructures for Research, Experimental  
195 Development and Innovations project "IT4Innovations National Supercomputing Center - LM2015070", project ID OPEN-13-21.



## References

- Baringer, M. O. and Larsen, J. C.: Sixteen years of Florida Current Transport at 27N, *Geophysical Research Letters*, 28, 3179–3182, 2001.
- Chave, A. D., Luther, D. S., Lanzerotti, L. J., and Medford, L. V.: Geoelectric field measurements on a planetary scale: oceanographic and geophysical applications, *Geophysical Research Letters*, 19, 1411–1414, 1992.
- 200 Cox, C. S., Filloux, J. H., and Larsen, J. C.: Electromagnetic studies of ocean currents and electrical conductivity below the ocean-floor, in: *The Sea*, pp. 637–693, 1971.
- Denig, W. F.: Geomagnetic kp and ap Indices, <http://www.ngdc.noaa.gov/stp/GEOMAG/kp{ }ap.html>, 2015.
- Faraday, M.: The Bakerian Lecture. Experimental Researches in Electricity. Terrestrial Magneto-electric Induction., *Philosophical Transactions of the Royal Society of London*, 122, 163–194, <https://doi.org/10.1098/rstl.1851.0001>, 1832.
- 205 Finlay, C. C., Maus, S., Beggan, C. D., Bondar, T. N., Chambodut, A., Chernova, T. A., Chulliat, A., Golovkov, V. P., Hamilton, B., Hamoudi, M., Holme, R., Hulot, G., Kuang, W., Langlais, B., Lesur, V., Lowes, F. J., Lühr, H., Macmillan, S., Manda, M., McLean, S., Manoj, C., Menvielle, M., Michaelis, I., Olsen, N., Rauberg, J., Rother, M., Sabaka, T. J., Tangborn, A., Tøffner-Clausen, L., Thébaud, E., Thomson, A. W. P., Wardinski, I., Wei, Z., and Zvereva, T. I.: International Geomagnetic Reference Field: the eleventh generation, *Geophysical Journal International*, 183, 1216–1230, <https://doi.org/10.1111/j.1365-246X.2010.04804.x>, <http://doi.wiley.com/10.1111/j.1365-246X.2010.04804.x>, 2010.
- 210 Flosadóttir, Á. H., Larsen, J. C., and Smith, J. T.: Motional induction in North Atlantic circulation models, *Journal of Geophysical Research*, 102, 10353–10372, 1997.
- Forget, G., Campin, J. M., Heimbach, P., Hill, C. N., Ponte, R. M., and Wunsch, C.: ECCO version 4: An integrated framework for non-linear inverse modeling and global ocean state estimation, *Geoscientific Model Development*, 8, 3071–3104, <https://doi.org/10.5194/gmd-8-3071-2015>, 2015.
- 215 Fujii, I. and Utada, H.: On Geoelectric Potential Variations Over a Planetary Scale, Ph.D. thesis, The University of Tokyo, 2000.
- Fukumori, I., Wang, O., Fenty, I., Forget, G., Heimbach, P., and Ponte, R. M.: ECCO Version 4 Release 3, Tech. rep., 2017.
- Grayver, A. V., Munch, F. D., Kuvshinov, A. V., Khan, A., and Sabaka, T. J.: Joint inversion of satellite-detected tidal and magnetospheric signals constrains electrical conductivity and water content of the upper mantle and transition zone, *Geophysical Research Letters*, 44, 6074–6081, <https://doi.org/10.1002/2017GL073446>, 2017.
- 220 Irrgang, C., Saynisch, J., and Thomas, M.: Ensemble simulations of the magnetic field induced by global ocean circulation: estimating the uncertainty, *Journal of Geophysical Research: Oceans*, 121, 1866–1880, <https://doi.org/10.1002/2016JC011633>.Received, 2016a.
- Irrgang, C., Saynisch, J., and Thomas, M.: Impact of variable seawater conductivity on motional induction simulated with an ocean general circulation model, *Ocean Science*, 12, 129–136, <https://doi.org/10.5194/os-12-129-2016>, 2016b.
- 225 Irrgang, C., Saynisch, J., and Thomas, M.: Utilizing oceanic electromagnetic induction to constrain an ocean general circulation model: A data assimilation twin experiment, *JAMES*, 2017.
- Koyama, T.: A study on the electrical conductivity of the mantle by voltage measurements of submarine cables, Ph.D. thesis, University of Tokyo, 2001.
- Lanzerotti, L. J., Thomson, D. J., Meloni, A., Medford, L. V., and MacLennan, C. G.: Electromagnetic study of the Atlantic continental margin using a section of a transatlantic cable, *Journal of Geophysical Research*, 91, 7417–7427, 1986.
- 230 Lanzerotti, L. J., Medford, L. V., Kraus, J. S., MacLennan, C. G., and Hunsucker, R. D.: Possible measurements of small-amplitude TID's using parallel, unpowered telecommunications cables, *Geophysical Research Letters*, 19, 253–256, 1992a.





- Lanzerotti, L. J., Sayres, C. H., Medford, L. V., Kraus, J. S., and MacLennan, C. G.: Earth potential over 4000 km between Hawaii and California, *Geophysical Research Letters*, 19, 1177–1180, 1992b.
- 235 Lanzerotti, L. J., Medford, L. V., MacLennan, C. G., and Thomson, D. J.: Studies of Large-Scale Earth Potentials Across Oceanic Distances, *AT&T Technical Journal*, pp. 73–84, 1995.
- Lanzerotti, L. J., Medford, L. V., MacLennan, C. G., Kraus, J. S., Kappenman, J., and Radasky, W.: Trans-atlantic geopotentials during the July 2000 solar event and geomagnetic storm, *Solar Physics*, 204, 351–359, 2001.
- Larsen, J. C.: Electric and Magnetic Fields Induced by Deep Sea Tides, *The Geophysical Journal of the Royal Astronomical Society*, 16,  
240 47–70, 1968.
- Larsen, J. C.: Transport measurements from in-service undersea telephone cables, *IEEE Journal of Oceanic Engineering*, 16, 313–318, <https://doi.org/10.1109/48.90893>, <http://ieeexplore.ieee.org/lpdocs/epic03/wrapper.htm?arnumber=90893>, 1991.
- Larsen, J. C.: Transport and heat flux of the Florida Current at 27°N derived from cross-stream voltages and profiling data: theory and observations, *Philosophical Transactions of the Royal Society of London. Series A: Physical and Engineering Sciences*, 338, 169–236,  
245 <https://doi.org/10.1098/rsta.1992.0007>, 1992.
- Larsen, J. C. and Sanford, T. B.: Florida current volume transports from voltage measurements, *Science*, 227, 302–304, 1985.
- Malin, S. R. C.: Separation of lunar daily geomagnetic variations into parts of ionospheric and oceanic origin., *The Geophysical Journal of the Royal Astroxnomical Society*, 21, 447–455, 1970.
- Manoj, C., Kuvshinov, A., Neetu, S., and Harinarayana, T.: Can undersea voltage measurements detect tsunamis?, *Earth, Planets and Space*,  
250 62, 353–358, <https://doi.org/10.5047/eps.2009.10.001>, <http://www.terrapub.co.jp/journals/EPS/abstract/6203/62030353.html>, 2010.
- Pedatella, N. M., Liu, H., and Richmond, A. D.: Atmospheric semidiurnal lunar tide climatology simulated by the Whole Atmosphere Community Climate Model, *Journal of Geophysical Research*, 117, 1–11, <https://doi.org/10.1029/2012JA017792>, 2012.
- Sabaka, T. J., Tyler, R. H., and Olsen, N.: Extracting ocean-generated tidal magnetic signals from Swarm data through satellite gradiometry, *Geophysical Research Letters*, 43, 3237–3245, <https://doi.org/10.1002/2016GL068180>.Received, 2016.
- 255 Šachl, L., Martinec, Z., Velínský, J., Irrgang, C., Petereit, J., Saynisch, J., Einšpigel, D., and Schnepf, N. R.: Modelling of electromagnetic signatures of global ocean circulation: physical approximations and numerical issues, *Earth, Planets and Space*, 71, <https://doi.org/10.1186/s40623-019-1033-7>, <https://doi.org/10.1186/s40623-019-1033-7>, 2019.
- Sanford, T. B.: Motionally induced electric and magnetic fields in the sea, *Journal of Geophysical Research*, 76, <https://doi.org/10.1029/JC076i015p03476>, <http://www.agu.org/pubs/crossref/1971/JC076i015p03476.shtml>, 1971.
- 260 Schnepf, N. R.: Going electric: Incorporating marine electromagnetism into ocean assimilation models, *Journal of Advances in Modeling Earth Systems*, 9, 1–4, <https://doi.org/10.1002/2017MS001130>, 2017.
- Schnepf, N. R., Nair, M., Maute, A., Pedatella, N. M., Kuvshinov, A., and Richmond, A. D.: A Comparison of Model-Based Ionospheric and Ocean Tidal Magnetic Signals With Observatory Data, *Geophysical Research Letters*, 45, 7257–7267, <https://doi.org/10.1029/2018GL078487>, 2018.
- 265 Shimizu, H., Koyama, T., and Utada, H.: An observational constraint on the strength of the toroidal magnetic field at the CMB by time variation of submarine cable voltages, *Geophysical Research Letters*, 25, 4023–4026, 1998.
- Sleijpen, G. L. G. and Fokkema, D. R.: BiCGstab(ell) for Linear Equations involving Unsymmetric Matrices with Complex Spectrum, *Electronic Transactions on Numerical Analysis*, 1, 11–32, 1993.
- Tyler, R. H., Maus, S., and Lühr, H.: Satellite observations of magnetic fields due to ocean tidal flow., *Science*, 299, 239–241,  
270 <https://doi.org/10.1126/science.1078074>, <http://www.ncbi.nlm.nih.gov/pubmed/12522247>, 2003.



- Tyler, R. H., Boyer, T. P., Minami, T., Zweng, M. M., and Reagan, J. R.: Electrical conductivity of the global ocean, *Earth, Planets and Space*, 69, <https://doi.org/10.1186/s40623-017-0739-7>, 2017.
- Vanyan, L. L., Utada, H., Shimizu, H., Tanaka, Y., Palshin, N. A., Stepanov, V., Kouznetsov, V., Medzhitov, R. D., and Nozdrina, A.: Studies on the lithosphere and the water transport by using the Japan Sea submarine cable (JASC): 1. Theoretical considerations, *Earth, Planets and Space*, 50, 35–42, <https://doi.org/10.1186/BF03352084>, 1998.
- 275
- Velímský, J.: Determination of three-dimensional distribution of electrical conductivity in the Earth's mantle from Swarm satellite data: Time-domain approach, *Earth, Planets and Space*, 65, 1239–1246, <https://doi.org/10.5047/eps.2013.08.001>, 2013.
- Velímský, J. and Martinec, Z.: Time-domain, spherical harmonic-finite element approach to transient three-dimensional geomagnetic induction in a spherical heterogeneous earth, *Geophysical Journal International*, 161, 81–101, <https://doi.org/10.1111/j.1365-246X.2005.02546.x>, 2005.
- 280
- Velímský, J., Šachl, L., and Martinec, Z.: The global toroidal magnetic field generated in the Earth's oceans, *Earth and Planetary Science Letters*, 509, 47–54, <https://doi.org/10.1016/j.epsl.2018.12.026>, 2019.



**Table 1.** The seafloor voltage cables used in this study. The HAW1N and S cables run parallel to each other.

Cable	Starting location	Ending location	Length (km)	Timespan
HAW1N&S	Point Arena, CA, USA	Hanauma Bay, HI, USA	3805	04/1990–12/2001
HAW3	Makaha, HI, USA	San Luis Obispo, CA, USA	3946	08/1994–07/2000
OKI	Okinawa, Japan	Ninomiya, Japan	1447	04/1999–12/2001

**Table 2.** The correlation coefficients ( $R$ ) and  $R^2$  values between the processed cable voltage data and numerical predictions of cable voltage.

Cable	30.5 day spline fit		90 day spline fit	
	$R$	$R^2$	$R$	$R^2$
HAW1N	-0.2675	0.0716	-0.3591	0.1290
HAW1S	-0.1540	0.0237	-0.1779	0.0316
HAW3	0.3129	0.0979	0.4111	0.1690
OKI	0.5920	0.3505	0.6526	0.4259

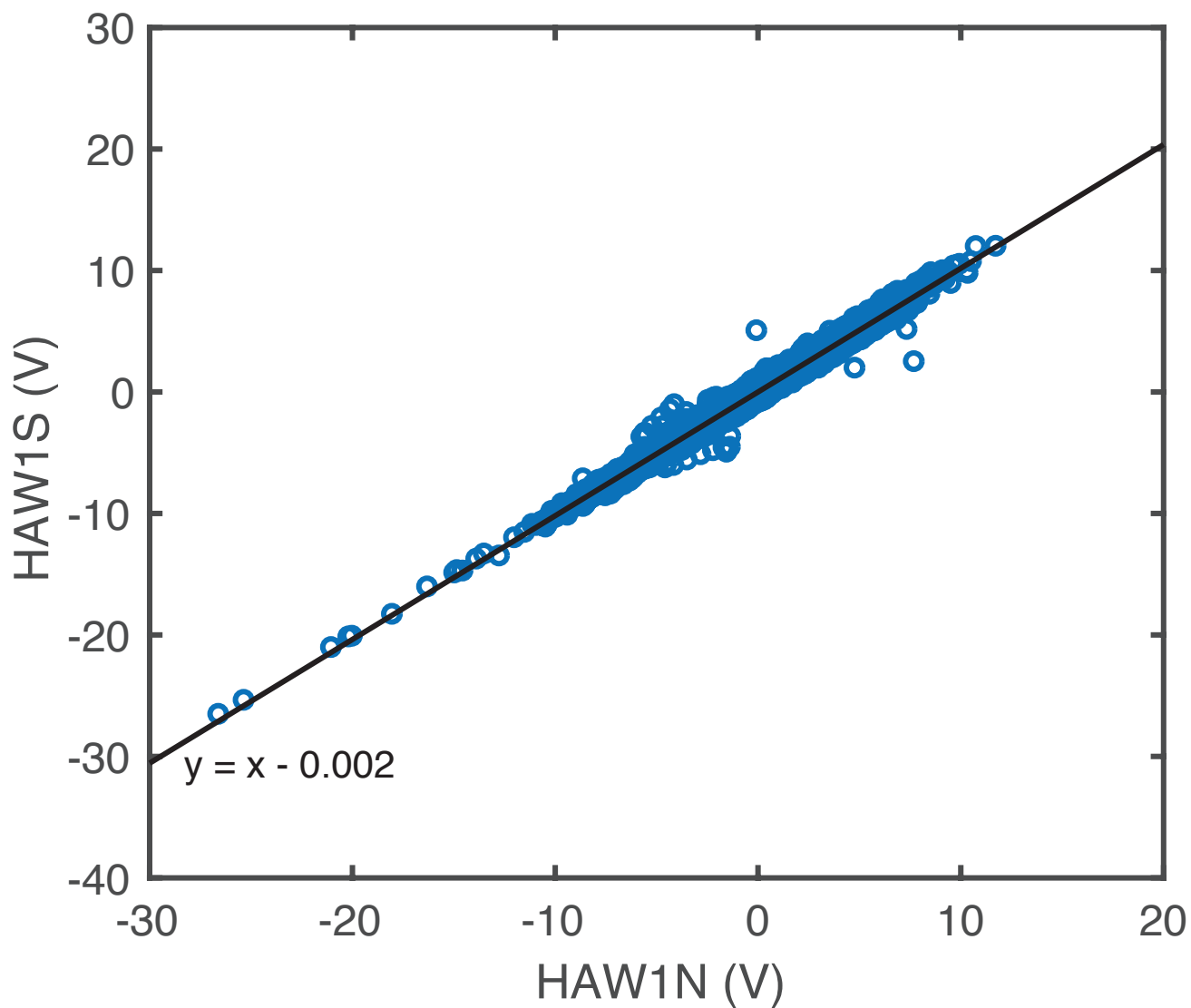


**Figure 1.** The voltage data of HAW1N versus HAW1S is shown in a correlation scatter plot. As shown by the line of best fit ( $y = x - 0.002$ ), the data from the two cables match very closely.

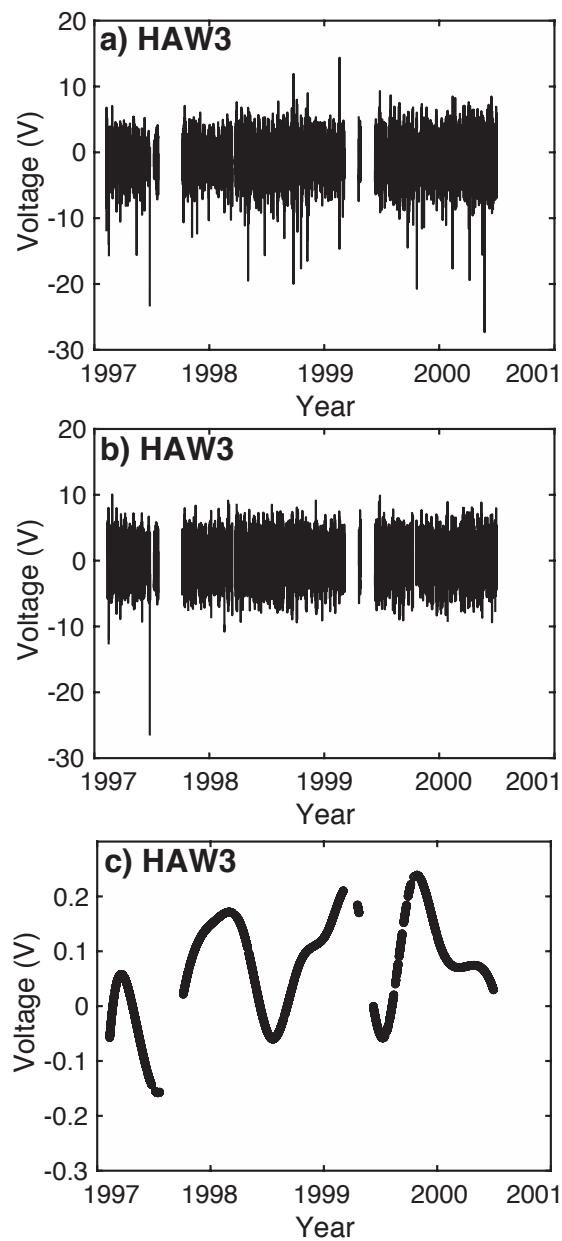


**Figure 2.** Each step of the data processing is shown here using HAW3 as an example: a) the raw time series, b) the time series with days of  $A_p > 20$  removed and tidal signals also removed, and c) the smoothed time series produced by splines with 90 day knots.

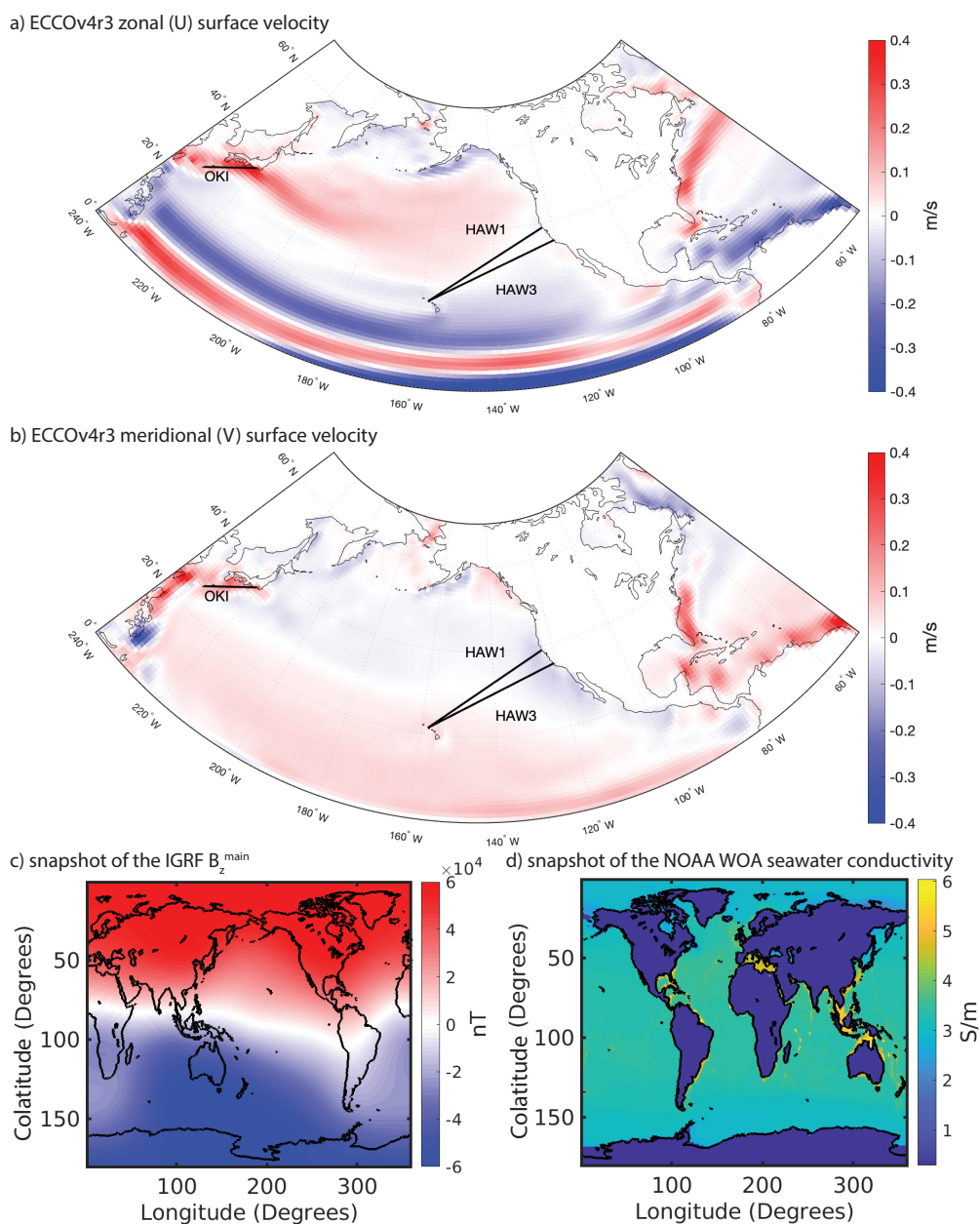


**Figure 3.** The surface velocities from ECCOV4r3 are shown in a) for the zonal (U) component and b) for the meridional (V) component. The labelled, thick black lines denote the sea floor voltage cables used in this study. A snapshot of the IGRF vertical main field,  $B_z^{main}$ , from January 17, 1997 is illustrated in c) and d) depicts the NOAA World Ocean Atlas seawater electrical conductivity's January climatology in the surface layer.

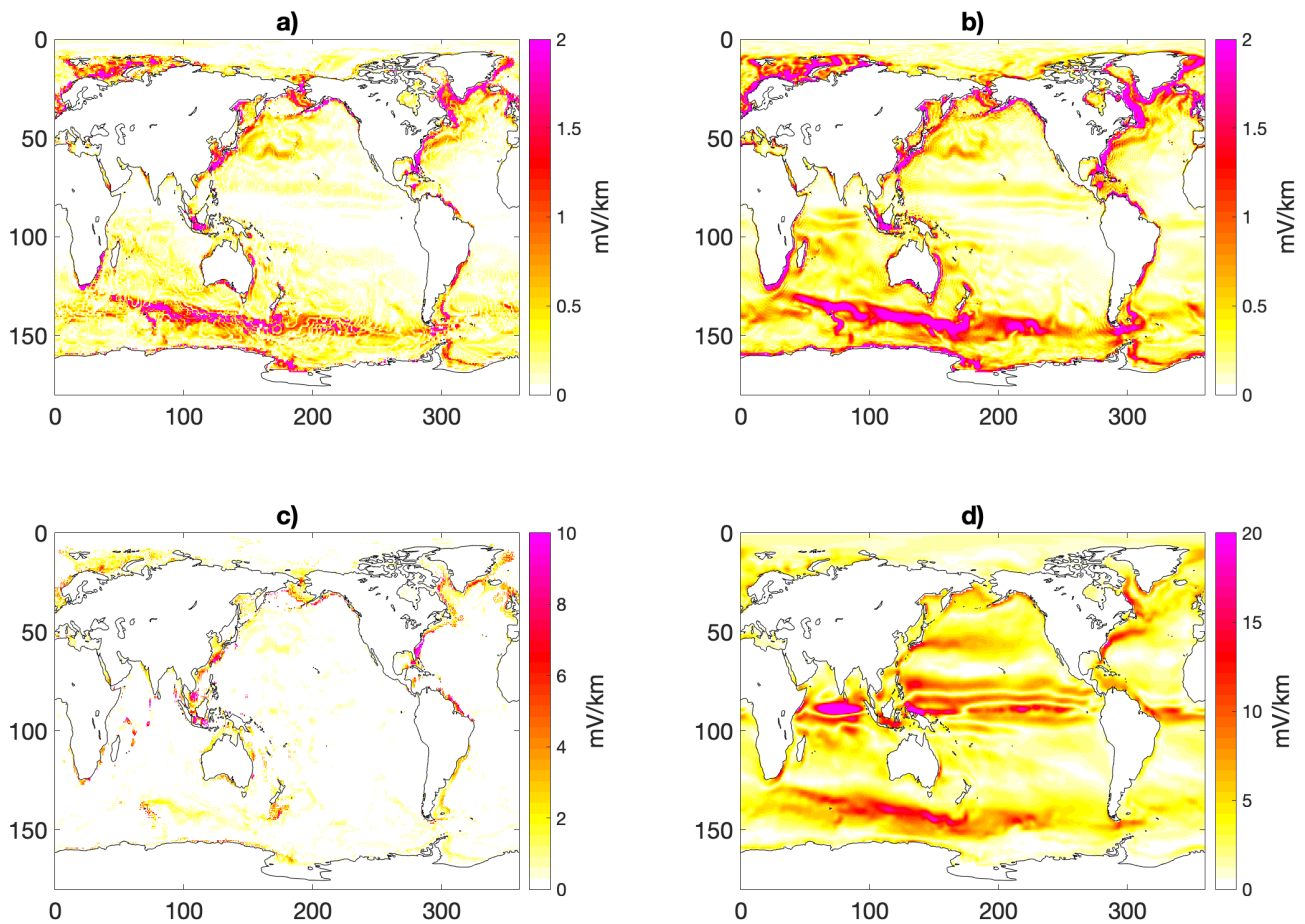


**Figure 4.** Maps of the predicted horizontal electric field's amplitude (i.e.  $|E_h|$ ) at the a) seafloor and b) sea surface, and maps of the total forcing (i.e.,  $|\mathbf{u} \times \mathbf{F}|$ ) at the c) seafloor and d) sea surface.

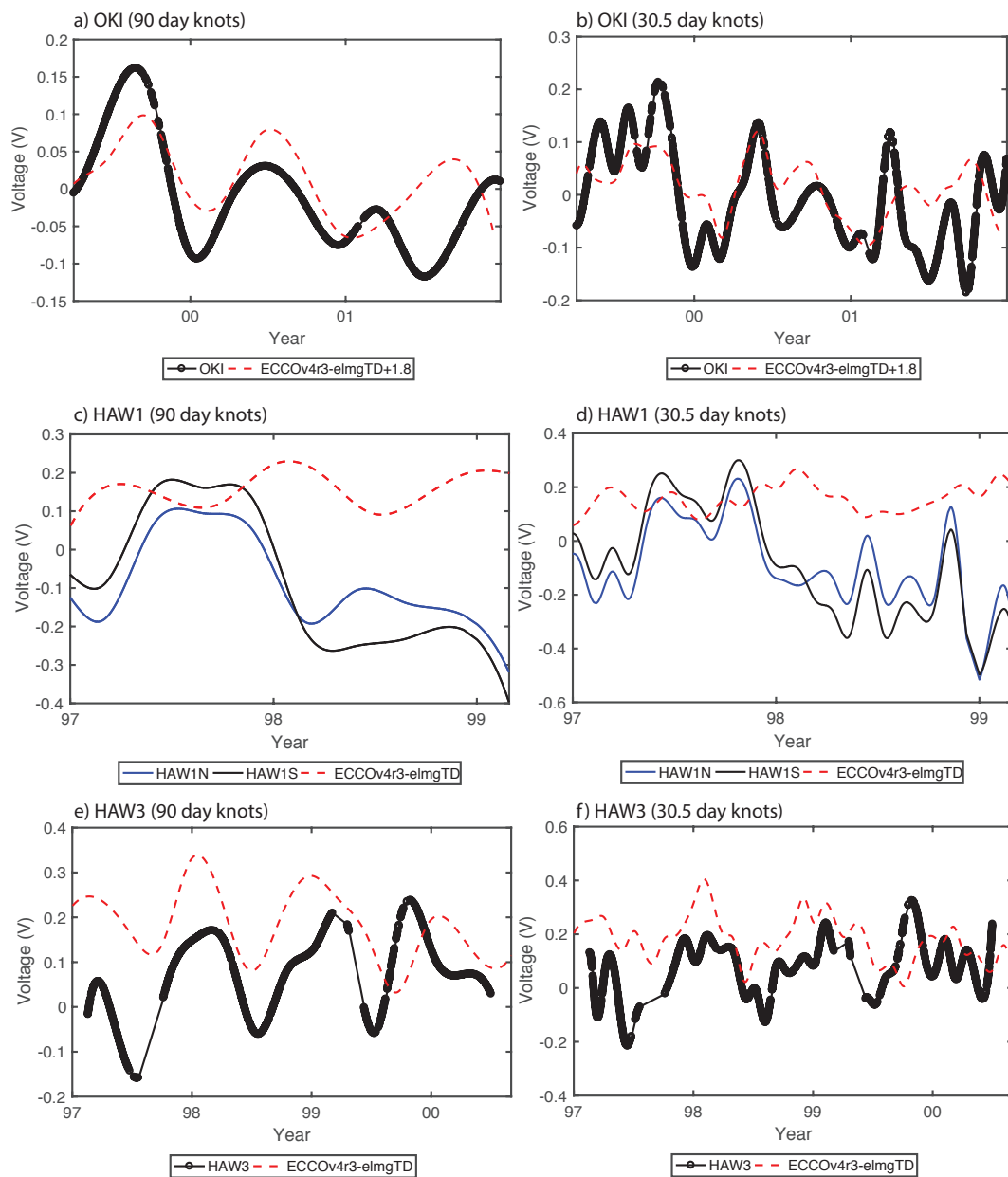


**Figure 5.** Shown here, for each cable, are the processed cable voltage data with a spline fit of 90 day knots (left column) and 30.5 day knots (right column) versus the numerical predictions corresponding to that cable.